Desalination and Water Treatment
www.deswater.com
doi: 10.5004/dwt.2020.24920

180 (2020) 349–359
March

A study of adsorption of Reactive Brilliant Red (K-2BP) by amino-modified macadamia nut shells

Qian Feng[a,b], Ran Ge[a,b], Yangyang Yu[c], Wen Yang[d], Jiashun Cao[a,b], Xindi Chen[e], Zhaoxia Xue[a,b], Fang Fang[a,b], Jingyang Luo[a,b], Jianfeng Ye[f,*]

[a]*Key Laboratory of Integrated Regulation and Resource Development on Shallow Lakes, Ministry of Education, Hohai University, Nanjing 210098, China, Tel. +86 25 83781619; emails: xiaofq@hhu.edu.cn (Q. Feng), sunrisegeran@163.com (R. Ge), Tel. +86 25 83786701; email: caojiashun@163.com (J. Cao), Tel. +86 25 83786701; email: xzhx223 @163.com (Z. Xue), Tel. +86 25 83781619; email: ffang65 @hhu.edu.cn (F. Fang), Tel. +86 25 83786701; email: luojy2016@hhu.edu.cn (J. Luo)*
[b]*College of Environment, Hohai University, Nanjing 210098, China*
[c]*Beifang Investigation, Design & Research CO.LTD, Tianjin 300222, China, Tel. +86 25 83781619; email: yuyy@hhu.edu.cn*
[d]*Central and Southern China Municipal Engineering Design & Research Institute CO.LTD., Wuhan 430010, China, Tel. +86 25 83781619; email: 904714138@qq.com*
[e]*College of Harbour, Coastal and Offshore Engineering, Hohai University, Nanjing 210098, China, Tel. +86 25 83781619; email: chenxindi1991@hhu.edu.cn*
[f]*Shanghai Academy of Environmental Sciences, Shanghai, P.R. China, Tel. +86 21 64085119, Fax: +86 21 64085119; email: yejf99@aliyun.com*

Received 5 May 2019; Accepted 13 September 2019

ABSTRACT

Macadamia nut shells (MNS), an abundant forestry residue rich in cellulose and lignin, were amino modified to adsorb reactive brilliant red (K-2BP). The raw MNS, and the ethylenediamine, diethylenetriamine and triethylenetetramine modified MNS (EMNS, DMNS, and TMNS) were characterized by scanning electron microscopy, laser particle sizer, Fourier transform infrared (FTIR) spectroscopy and thermogravimetric analysis. The effect of pH on the adsorption process of K-2BP was studied and combined with the zeta potential analysis. The adsorption mechanism was explained. The K-2BP dye adsorption capacity decreased as pH increased. Results showed that TMNS had the highest adsorption capacity due to a higher pH_{PZC} which implied a more positive surface charge and more amine and secondary amine on the surface. Thermodynamic analysis verified that the adsorption process was endothermic and spontaneous. The adsorption kinetics of these modified adsorbents was well matched with pseudo-second-order equation, indicating that the adsorption process is chemical adsorption. The Langmuir and Freundlich isotherm models were used to describe the adsorption processes of K-2BP dye onto four kinds of adsorbents. The Freundlich model showed the best statistics, which meant the adsorption of K-2BP onto adsorbents from the aqueous solutions was constant with a monolayer formation.

Keywords: Macadamia nut shell; Dye adsorption; Reactive Brilliant Red; Amino modification

* Corresponding author.

1. Introduction

The extensive use and direct discharge of dyes without treatments have caused severe environmental and health problems [1]. Azo dyes are the most widely used dyes, which account for over 60% of the total number of dyes known to be manufactured [2]. Among several removal methods for azo dyes in aqueous solution, such as adsorption [3,4], coagulation [5], and advanced oxidation [4], the adsorption has attracted most attention since it is economical, efficient, easy to conduct [6,7] and has high adsorption capacity.

Macadamia nut shells (MNS), an abundant forestry residue rich in cellulose and lignin, have been utilized to produce value-added activated carbons (ACs) [8]. Therefore, waste adsorption on ACs from MNS has aroused extensive attention in the past few decades. For instance, the adsorption capacity of MNS-derived ACs to phenol (341 mg/g) is significantly higher than that of commercial ACs (32 mg/g) [9]. Poinern et al. [10] reported the high-efficient aurocyanide adsorption on MNS-derived ACs. ACs converted from NaOH-modified MNS have also been used for tetracycline removal [11]. In addition, various chemical-modified MNS-derived ACs have been successfully applied to the removal of hexavalent chromium [12], reactive blue [13] and methylene blue [14]. However, ACs production is restricted due to its energy and capital-intensive process involving carbonization and activation.

Compared with original ACs, modified MNS ACs are economical, energy-efficient, and easy to regenerate with high efficiency [8,15]. Surface functionalities of carbon material can anchor organic molecules and bind with heavy metals, consequently increasing the removal efficiency of pollutants [16]. A considerable number of functional groups, such as amino, nitro, hydroxyl, carboxyl, etc., have been tested as the chemical modifications to alter the surficial properties [17,18]. Compared with other surface functionalities, amino shows more potential to strengthen the adsorption of metal ions and dyes. Yang and Jiang [19] reported that adsorption capacity of amino-functionalized biochar to copper (II) was significantly higher than that of untreated biochar. Ma et al. [20] demonstrated that the adsorption capability of modified biochar to Cr (V) was 20 times higher than that of original biochar. In another study, Cao et al. [21] reported that the azo dyes removal rate by NaOH- and DETA-modified walnut shells was nearly 10 times higher than that before modification. Although many studies have revealed the adsorption of heavy metals onto amino-modified MNS material, dye adsorption has been rarely studied. Also, the kinetics and thermodynamics of dye adsorption on amino-modified MNS need to be further studied.

In this study, MNS was modified by ethylenediamine, diethylenetriamine and triethylenetetramine to adsorb reactive brilliant red (K-2BP). The morphology of MNS was characterized and compared by scanning electron microscope and laser granulometer before and after amino treatment. The amino modification of MNS was qualified by Fourier transform infrared (FTIR) spectroscopy. The thermal stability of adsorbents was analyzed using thermogravimetric analysis (TGA). The influences of pH on the adsorption process were investigated. The adsorption mechanism was explained with zeta potentiometric analysis. In addition, the adsorption characteristics and mechanism of dye adsorption process were further studied by using thermodynamics, adsorption kinetics and adsorption isotherms.

2. Materials and methods

2.1. Materials

Ethylenediamine, diethylenetriamine and triethylenetetramine were obtained from KeLong Chemical Co. Ltd. (China). Reactive brilliant red (K-2BP) ($C_{25}H_{14}C_{l2}N_7Na_3O_{10}S_3$, molecular weight of 808.48 g/mol) was purchased from Jinan Xinxing Dye Chemical Co. Ltd. (China) (Fig. 1 for the chemical structures of different chelating ligand and reactive brilliant red).

2.2. Synthesis of modified MNS

The pristine macadamia nut shells were initially soaked in distilled water to remove surface-attached particles and water-soluble materials. The residual pulp was cleared by blades and brushes and dried at 105°C for 24 h, and then crushed to powder (120 mesh) and stored in a drying bottle for further analysis and modification. 2 g of MNS and different modifiers (ethylenediamine, diethylenetriamine and triethylenetetramine) were mixed and stirred with magnetic stirrer at 70°C for 180 min separately. After that, three modified adsorbents were rinsed in deionized water till the pH of leachate reached 7. The modified adsorbents were dried at 60°C before use.

2.3. Adsorption experiment

The adsorption of K-2BP was carried out in 100 mL Erlenmeyer flasks by adding 0.13 mol EMNS, DMNS and TMNS, to 50 mL K-2BP solution, respectively. The pH was adjusted by adding HCl (0.1 mol/L or 1 mol/L) or NaOH (0.1 or 1 mol/L). All the Erlenmeyer flasks were then agitated in a shaking incubator (180 rpm, 120 min). The solution interacted with adsorbent was then filtered through a 0.45 μm filter, and the concentration of the filtrate was quantified by UV-VIS spectrometer at the maximum wavelength of 538 nm.

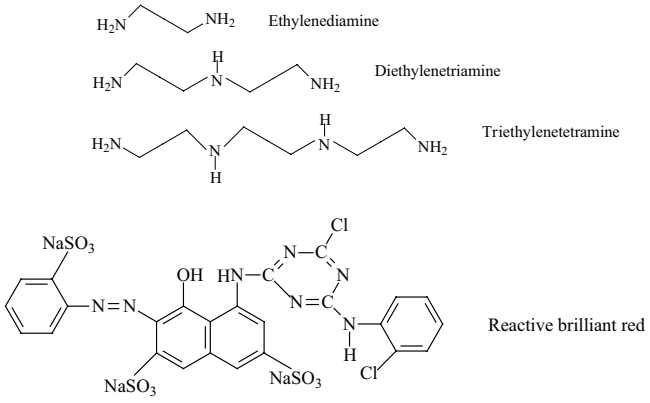

Fig. 1. Chemical structures of different chelating ligand and reactive brilliant red.

2.4. Analytic methods

The concentration of residual dyestuff was quantified by UV-VIS spectrometer (ALPHA-1506, China) [22]. The morphology of the adsorbents was characterized by scanning electron microscope (HITACHI-S-4800N, Japan) [23]. The particle size distribution of different adsorbents was studied by Malvern particle size analyzer (SEDIMAT 4-12, Germany). The surface functional groups and chemical bonds of the adsorbents were characterized by FTIR spectroscopy (Nexus 870, USA) [24]. The thermal stabilities of the adsorbents were studied by TGA (Pyris 1 DSC, USA) [25].

2.5. Calculations

The adsorption capacity and removal efficiency (%) of the adsorbents were determined by the following equations [26,27]:

$$q_{e,t} = \frac{(C_0 - C_t) \times V}{W} \tag{1}$$

$$K - 2\text{BP}\% = \frac{C_0 - C_t}{C_0} \times 100\% \tag{2}$$

where C_0 (mg/L) represents the initial dye concentration, C_t (mg/L) represents the dye concentration at time t, V (L) represents the solution volume, W (g) represents the adsorbent mass, $q_{e,t}$ (mg/g) represents the amount of dye adsorbed by adsorbent at time t.

3. Results and discussion

3.1. Characterization of modified adsorbent

3.1.1. SEM image analysis and aperture size

The porous nature and surface structure of the pristine adsorbent (MNS), modified adsorbents (EMNS, DMNS, TMNS) and TMNS after adsorption (named as K-TMNS) were examined using SEM. According to Fig. 2a, MNS is multilayer and tubular structure with a few cracks presenting as porous. After modification, the multilayer surfaces of the adsorbents became smooth due to organic modifiers linkage during the chemical modification [28]. The surface morphology of the adsorbents was obviously changed after K-2BP adsorption. The original layered structure (Fig. 2d) became blurred after adsorption (Fig. 2e). With the increase of adsorption capacity, the surface of TMNS layered structure

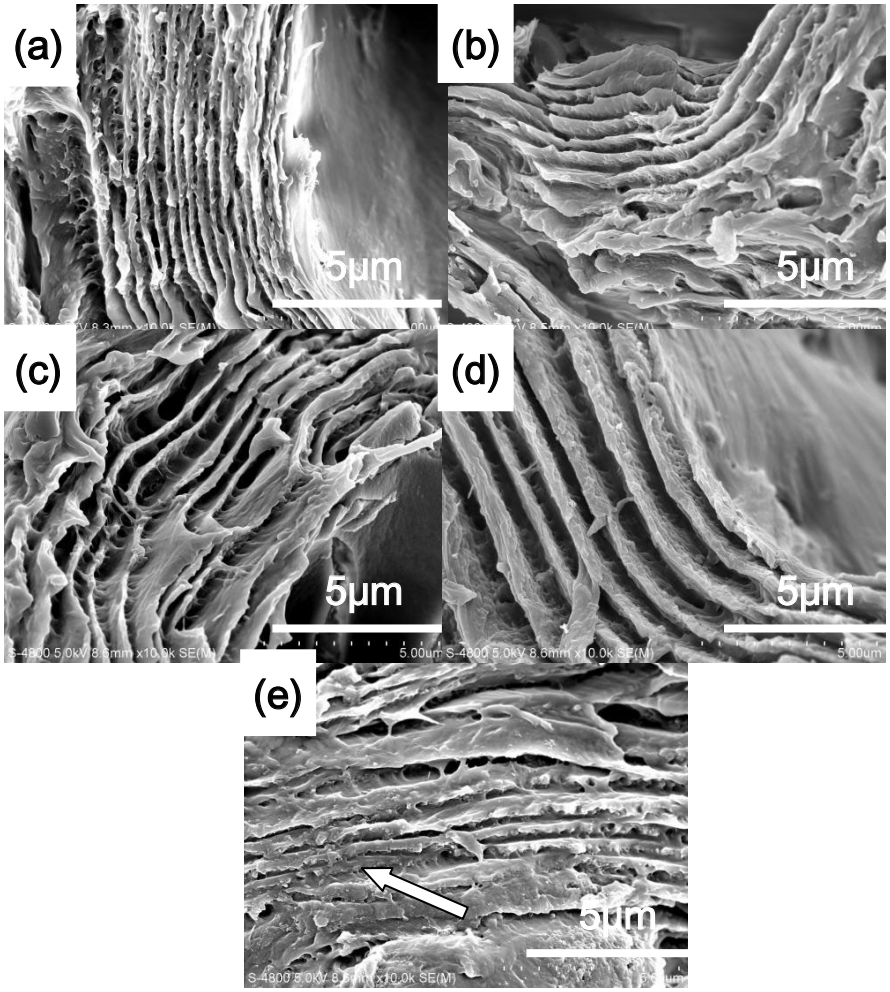

Fig. 2. SEM micrographs of (a) MNS, (b) EMNS, (c) DMNS, (d) TMNS, and (e) K-TMNS.

shows an agglomeration trend, as depicted by the arrows in Fig. 2e. Less stratified structure was found as the amino numbers in modifiers increased (Figs. 2b–d).

As shown in Fig. 3, the specific surface area, total pore volume of pristine adsorbent and modified adsorbents varied considerably. The specific surface area and total pore volume decreased. The mean particle size for MNS, EMNS, DMNS and TMNS were 84.497, 109.098, 121.400 and 113.006 μm, respectively. Mean particle size of EMNS, DMNS and TMNS was larger than MNS because the rinse process drained a part of small size adsorbents (Fig. 4). Increasing amino numbers of modifiers resulted in the decrease of specific surface area and total pore volume, which might be due to the steric hindrance of grafted functional group to the diffusion of nitrogen into interior of MNS [29].

3.1.2. FTIR analysis

The FTIR spectroscopy was used to detect if the dyes successfully attached to any groups of the modified nut shell and the groups that the K-2BP dye tended to attach. The spectrum of the pristine MNS (Fig. 5) exhibited a strong peak at 3,403 cm^{-1}, representing the O–H stretching vibration of hydroxyl groups or adsorbed water of cellulose and lignin [30,31]. The bands at around 2,902 cm^{-1} were attributed to C–H stretching vibrations, while the band at around 1,375 cm^{-1} in methyl and methylene groups was caused by the C–H in-plane bending vibrations [32,33]. The bands at around 1,739 cm^{-1} were resulted from C=O stretching vibrations in the carboxyl group [34,35]. The bands near 1,465 and 1,512 cm^{-1} were assigned to C=C stretching that can be attributed to the presence of aromatic or benzene rings in lignin [2,36]. The band at 1,033 cm^{-1} shows C–O stretching in carboxyl acids, alcohols and phenols [37,38]. Fig. 5 also gives the FTIR spectra of the modified adsorbents (curves EMNS, DMNS, TMNS) and the adsorption of K-2BP by adsorbents (curves K-MNS, K-EMNS, K-DMNS, K-TMNS). After chemical modification reaction, a strong broad band appeared in the range of 3,200–3,600 cm^{-1}, mainly from the N–H stretching vibration (overlapped by O–H) [39]. A new strong band of the modified adsorbents appeared in the range of 1,651–1,641 cm^{-1} due to the C=O stretching vibrations coming

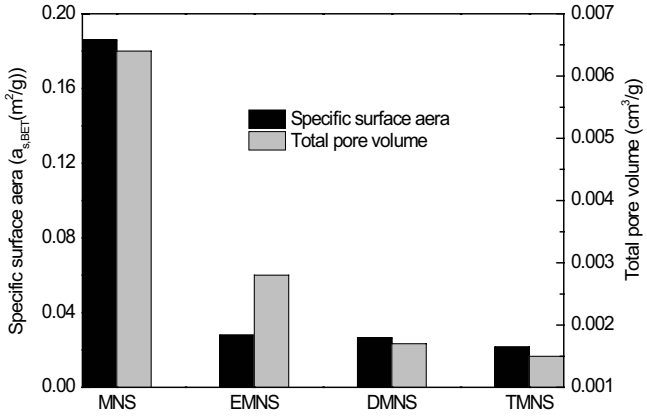

Fig. 3. Specific surface area, total pore volume of MNS, EMNS, DMNS and TMNS.

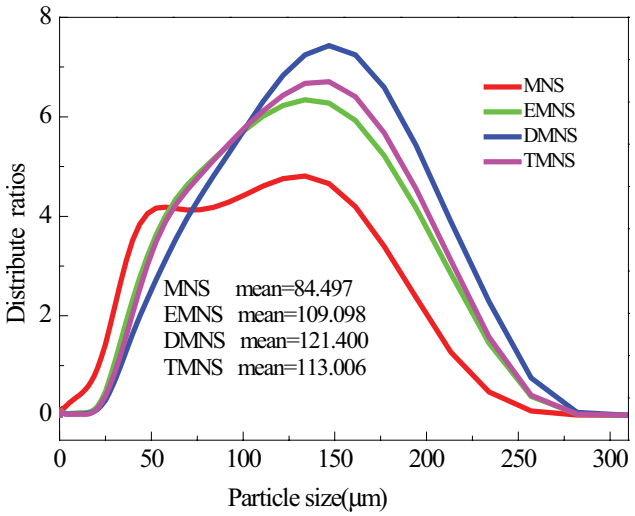

Fig. 4. Particle size distribution of MNS, EMNS, DMNS and TMNS.

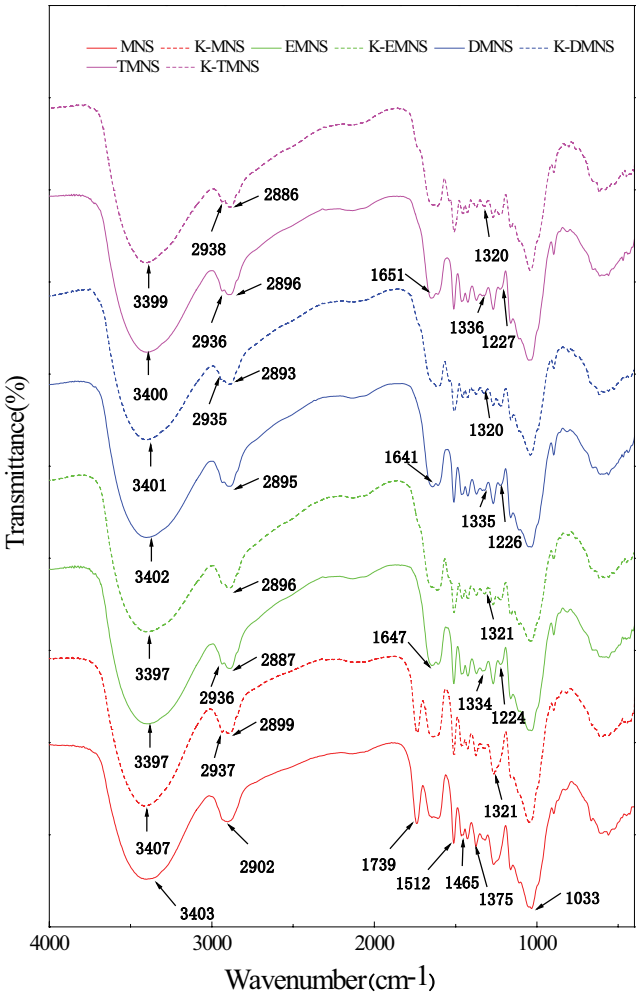

Fig. 5. FTIR spectra of four adsorbents and the adsorbents after K-2BP adsorption, respectively.

from the amide group [40]. The new band generated at 1,335 and 1,225 cm^{-1} can be ascribed to C–N bend vibrations in the amino group and amide group, respectively, indicating that many amine groups were grafted on the surface of MNS after condensation polymerization [41–43], in accordance with the results in section 3.1.1. The C–N band near 1,334 cm^{-1} shift to 1,320 cm^{-1} after adsorption due to the K-2BP occupation. Therefore, the FTIR results demonstrated the main functional groups of the pristine macadamia nut shell were hydroxyl and carboxyl. The amino groups were grafted onto the surface of the pristine macadamia nut shell because of acylated condensation reaction between the amino groups and the carboxyl groups [35]. Additionally, the K-2BP dye molecules were adsorbed on the modified adsorbents with amino groups.

3.1.3. Thermogravimetric analysis

The thermal stability of MNS, EMNS, DMNS, TMNS was investigated by TGA. All TGA tests were conducted at 30°C to 600°C with an increase rate of 20°C/min under air atmosphere (Fig. 6). The weight loss of 11.88 wt% was observed at 100°C due to the removal of physically adsorbed water from the sample [32,44]. Similarly, the weight loss of 9.78 wt%, 5.67 wt%, 6.75 wt% at 100°C was obtained for EMNS, DMNS, TMNS, respectively. The quality of modified adsorbent decreased more slowly than that of MNS because of low humidity of modified adsorbents caused by chemical modifications. The weight loss was around 50 wt% at 260°C–380°C during the main degradation, corresponding to the cellulose degradation [45]. The weight loss above 380°C could be attributed to the ring-opening reaction as well as the formation of crosslinked and condensed aromatic structures in lignin at high temperatures [46]. The TGA tests of MNS, EMNS, DMNS, TMNS indicated that they are thermally stable for dye removals under mild conditions.

3.2. Influence of pH on K-2BP dye removal

pH value is a very crucial parameter affecting the adsorption efficiency of K-2BP dye. The adsorptions of K-2BP dye by MNS, EMNS, DMNS and TMNS were investigated in a pH range of 2–10.

According to Fig. 7, the adsorption capacity of K-2BP dye decreased when pH value varied from 2 to 10. The maximum adsorption capacities of EMNS, DMNS and TMNS on K-2BP dye at pH = 2 was 282.15, 395.07 and 426.22 mg/g, respectively. It was clear that the adsorption capacities of EMNS, DMNS and TMNS were 2.55, 3.57 and 3.85 times higher than that of MNS, respectively. This could be attributed to zeta potential changes in surface electric charges of the three kinds of adsorbents.

As shown in Fig. 8, the zeta potentials of MNS, EMNS, DMNS and TMNS were 4.13, 7.83, 8.07 and 8.08, respectively. The surface charges of adsorbents were positive at

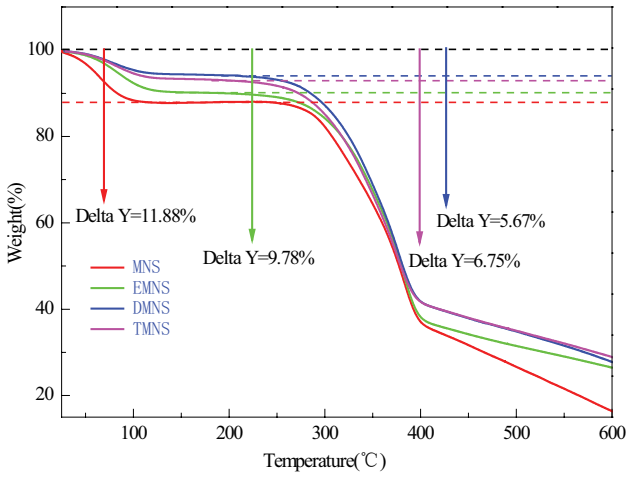

Fig. 6. TGA diagram of MNS, EMNS, DMNS and TMNS.

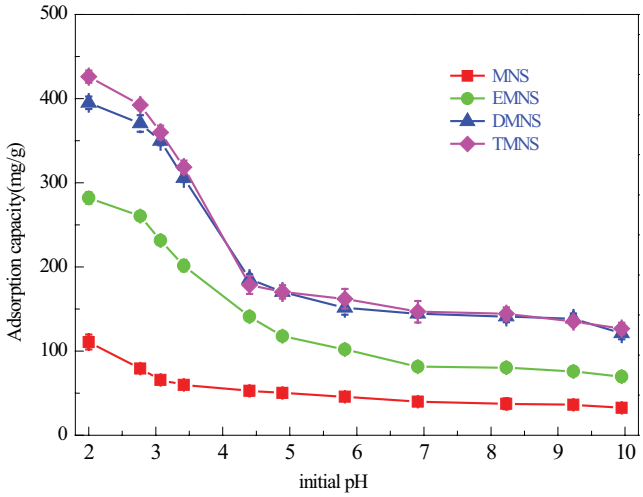

Fig. 7. Effects of pH on K-2BP adsorption by the adsorbents (MNS, EMNS, DMNS and TMNS) (conditions: temperature, 25°C; adsorbent dosage, 0.025 g; stirring rate, 180 rpm; reaction time, 180 min; initial dye concentration, 250 mg/L).

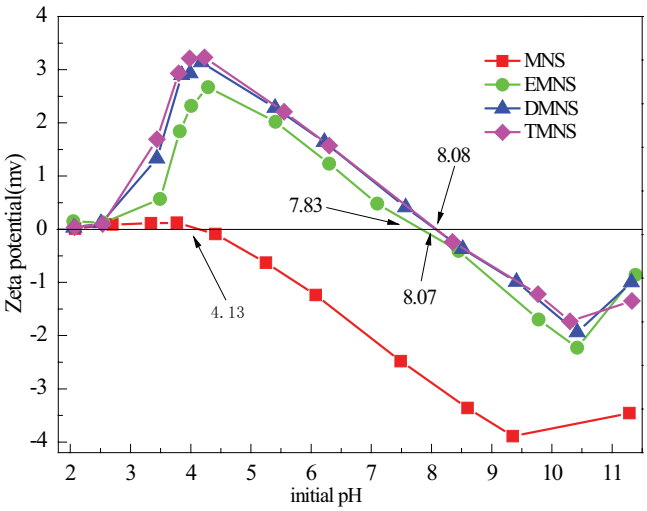

Fig. 8. Zeta potential curves for adsorbents (MNS, EMNS, DMNS and TMNS) as a function of pH (conditions: temperature, 25°C; adsorbent dosage, 0.025 g; stirring rate,180 rpm; reaction time, 180 min; initial dye concentration, 250 mg/L).

pH < pH_{PZC} and negative at pH > pH_{PZC}. Compared with the other adsorbents, TMNS possessed a higher pH_{PZC} implying that it had a more positive surface charge and more K-2BP dye could be adsorbed [47].

The adsorption mechanism can be explained by the electrostatic adsorption and the hydrogen bonding between amino, secondary amine, hydroxyl groups and dyes distributed on the surface of adsorbents (Fig. 9). Many functional groups such as amine, hydroxyl and carbonyl groups are distributed on the surface of the modified adsorbents. The predominant charges on the adsorbents surface at acidic pH were positive because lower pH led to a higher concentration of hydrogen ion in the solution, resulting in more amine, secondary amine and hydroxyl group protonated [48]. These protonated groups ($–NH_3^+$) resulted in the adsorbents possessing positive charges which can interact with the sulfonic acid groups of the K-2BP dyes through electrostatic adsorption [21,49,50]. By contrast, as pH increased, the negative charge on the adsorbents surface increased, and it starts to deprotonate, reducing electrostatic attraction and increasing electrostatic repulsion, leading to the decline of adsorption capacity. By the theory of electrostatic adsorption, the phenomenon presented in Fig. 7 can be well explained. That is to say, TMNS with more amino, secondary amine has the strongest adsorption capacity and the adsorption capacity decreased faster when pH increased (pH 3–4) [51,52]. Besides, the adsorption before amino modification indicated the inter-molecular interaction was involved. The adsorption was enhanced by the strong hydrogen bonding between K-2BP dye and the adsorbents which was a result of the strong combination of hydrophilic functional groups between the dye and the adsorbents [53,54].

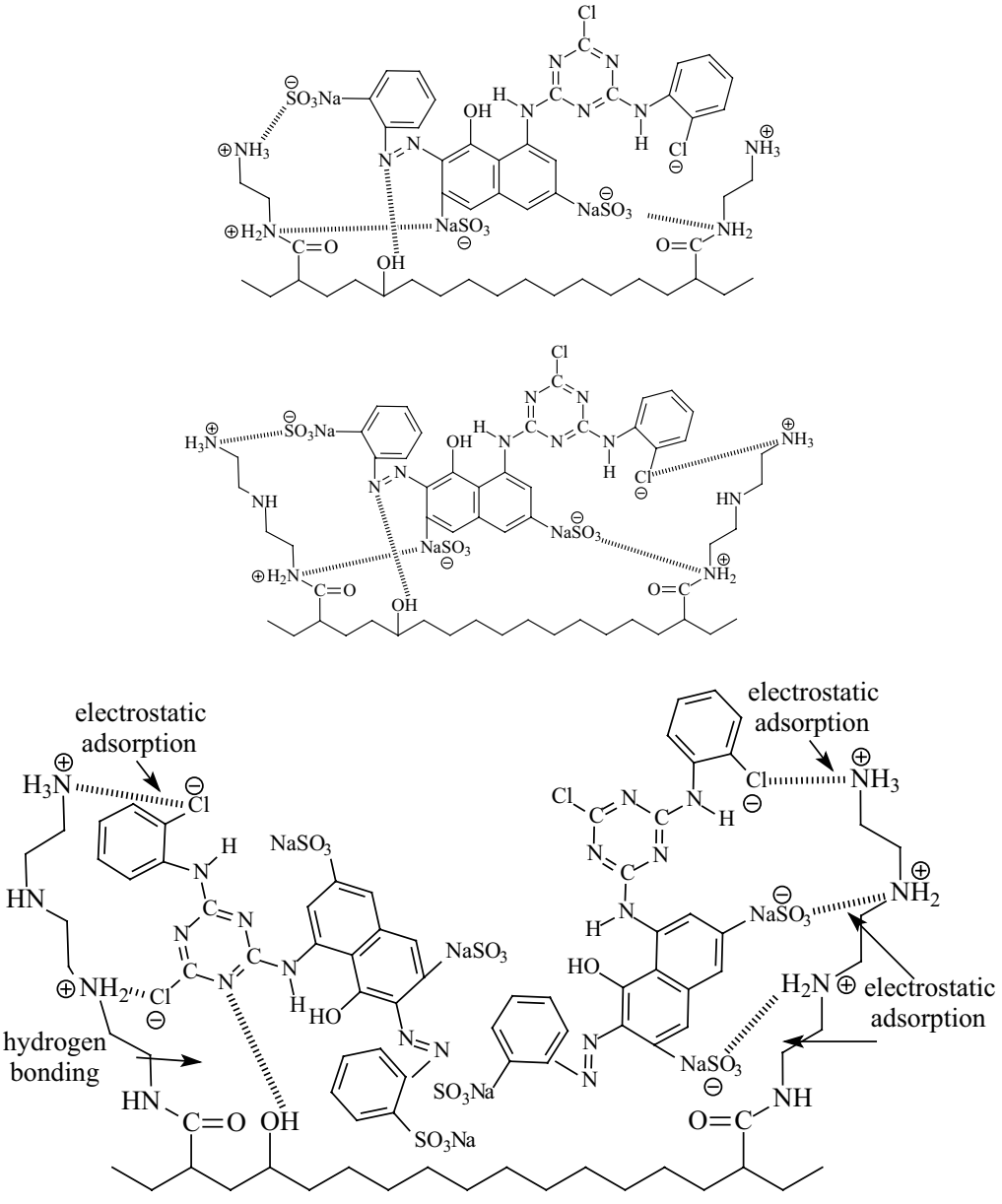

Fig. 9. Mechanism of interaction between K-2BP dye molecules and EMNS, DMNS, TMNS, respectively.

3.3. Thermodynamic studies

The adsorption thermodynamics is critical for the interpretation of adsorption mechanisms. The thermodynamic parameters such as the Gibbs free energy ($\Delta G°$), enthalpy change ($\Delta H°$) and entropy change ($\Delta S°$) were investigated by studying the sorption process at three different temperatures (293 K, 303 K and 313 K) [55–58]. The Van't Hoff equation was used to calculate these variables [59]:

$$\Delta G° = \Delta H° - T\Delta S° \tag{3}$$

$$\ln K_C = \frac{\Delta S°}{R} - \frac{\Delta H°}{RT} \tag{4}$$

$$K_C = \frac{q_e}{C_e} \tag{5}$$

where K_C is the adsorption equilibrium constant, which is the ratio of adsorbed K-2BP dye concentration to the dye concentration in solution at equilibrium. q_e is the amount of K-2BP dye adsorbed per unit mass of adsorbents (mg/g), C_e is the equilibrium K-2BP dye concentration in solution (mg/L), T is the absolute solution temperature (K) and R is the universal gas constant (8.314 J/mol K).

All the adsorption thermodynamic parameters of K-2BP dye adsorption on four kinds of adsorbents are summarized in Table 1.

The increase of K_C and the positive value of $\Delta H°$ revealed that the adsorption was an endothermic process [60]. Higher temperature increased the mobility of the dye molecules and the number of active sites for the adsorption [59]. Moreover, the positive value of $\Delta S°$ indicated the increasing randomness at the adsorbents/solution interface during the K-2BP dye adsorption process on the four kinds of adsorbents [19]. On the other hand, the negative $\Delta G°$ values were observed at all three temperatures, confirming that the adsorption of K-2BP dye was spontaneous. The decrease in $\Delta G°$ values with increasing temperature revealed that the adsorption was favorable at higher temperature [61,62].

3.4. Adsorption kinetics

The pseudo-first-order kinetic model and pseudo-second-order models (Eqs. (6) and (7)) are the noted models to research the adsorption kinetics with the experimental data for the adsorption of K-2BP dye by four kinds of adsorbents [3,48].

$$\ln(q_e - q_t) = \ln q_e - k_1 t \tag{6}$$

$$\frac{t}{q_t} = \frac{1}{k_2 q_e^2} + \frac{t}{q_e} \tag{7}$$

$$h = k_2 q_e^2 \tag{8}$$

where q_e (mg/g) and q_t (mg/g) are the amounts of K-2BP dye for adsorbents at equilibrium and at any time t (min), respectively. k_1 (1/min) is the adsorption equilibrium rate constant of pseudo-first-order kinetic model. k_2 (g/(mg min)) is the adsorption equilibrium rate constant of pseudo-second-order kinetic model. h (mg/g min) was used to calculate the initial adsorption rate constant.

The calculated parameters of the pseudo-first-order and pseudo-second-order models have been summarized in Table 2.

According to Table 2, the experimental data of four kinds of adsorbents demonstrated that the pseudo-second-order kinetics model achieved a larger correlation coefficient and the theoretical Q_e values were closer to the experimental $q_{e,cal}$ values than that of the pseudo-first-order model, which indicated that chemical adsorption, involving the electrostatic interaction and the hydrogen bonding between K-2BP dye and adsorbents, was the main control process of the four kinds of materials [19,63]. The rate constants (k_2) for K-2BP dye adsorption onto the EMNS, DMNS and TMNS were lower than that of the MNS. This indicated that they were slower to reach a specific fractional adsorption [64]. The high h value confirmed that the adsorption of K-2BP dye may be carried out via surface exchange reactions until the surface functional sites were occupied [21,65]. The chemical

Table 1
Thermodynamic parameters of adsorption of K-2BP on adsorbents (MNS, EMNS, DMNS, TMNS) (conditions: stirring rate, 180 rpm; reaction time, 180 min; initial dye concentration, 250 mg/L; pH, 6.91)

	Temperature (K)	K_C (L/mol)	$\Delta H°$ (kJ/mol)	$\Delta S°$ (J/(mol K))	$T\Delta S°$ (kJ/mol)	$\Delta G°$ (kJ/mol)	R^2
MNS	293	0.054067	0.00002	0.0029	0.00085	–0.00083	0.9817
	303	0.089185			0.00088	–0.00086	
	313	0.18981			0.00091	–0.00089	
EMNS	293	0.1388	0.00003	0.0028	0.00082	–0.00079	0.9949
	303	0.195499			0.00085	–0.00082	
	313	0.294942			0.00088	–0.00095	
DMNS	293	0.203284	0.00003	0.0031	0.00091	–0.00088	0.9235
	303	0.40264			0.00094	–0.00091	
	313	0.411023			0.00097	–0.00094	
TMNS	293	0.283213	0.00004	0.0030	0.00088	–0.00084	0.9356
	303	0.426174			0.00091	–0.00087	
	313	0.490182			0.00094	–0.00090	

Table 2
Kinetic parameters for the adsorption of K-2BP on adsorbents (MNS, EMNS, DMNS and TMNS) with different models (conditions: temperature, 25°C; stirring rate, 180 rpm; initial dye concentration, 250 mg/L; pH, 6.91)

Total number of amino groups (mol)		Q_e (mg/g)	Pseudo-first-order kinetic model			Pseudo-second-order kinetic model			
			$q_{e,cal}$ mg/g	k_1 min^{-1}	R^2	$q_{e,cal}$ mg/g	h mg/(g min)	k_2 g/(mg min)	R^2
	MNS	40.9412	65.7895	0.0152	0.9672	45.4545	0.9626	0.0004	0.9807
0.13 × 4 = 0.52	EMNS	81.4821	113.9546	0.0196	0.9386	84.0336	1.1693	0.0002	0.9896
0.13 × 6 = 0.80	DMNS	144.4762	131.4465	0.0227	0.9443	144.9275	5.5897	0.0003	0.9833
0.10 × 8 = 0.80	TMNS	146.8235	112.0449	0.0182	0.9561	151.5152	5.9488	0.0003	0.9918

modification process involving main reactions and number of amino groups carried by adsorbents is shown in Fig. 10.

Generally, adsorption capability of the macadamia shell increased after modified by amino. When the total numbers of amino modifying were the same, the adsorption equilibrium rates reached the same constant value. If the amino numbers were different, less time was needed to get the adsorption equilibrium rate constant for the modifiers with more amino numbers per mole. The variation in h values indicated that the initial adsorption rate could be higher by increasing the amino groups in per mol modifiers. As a result, macadamia shell modified with more amino groups showed a better performance in removing azo dye reactive brilliant red K-2BP in printing and dyeing wastewater.

3.5. Adsorption isotherms

In this study, the Langmuir and Freundlich isotherm models were used to describe the adsorption processes of K-2BP dye onto four kinds of adsorbents. The Langmuir model described an adsorption process that occurred upon a homogeneous surface where the adsorbate was distributed in monolayers. The Freundlich isotherm model was valid for multilayer adsorption of heterogeneous surface with a non-uniform distribution of heat of adsorption over the surface [33,66]. Langmuir and Freundlich isotherm models can be calculated by Eqs. (9) and (10).

$$\frac{C_e}{q_e} = \frac{1}{K_L Q_m} + \frac{C_e}{Q_m} \tag{9}$$

$$\ln q_e = \ln K_F + \frac{\ln C_e}{n} \tag{10}$$

where C_e (mg/L) is the ultimate concentration of K-2BP dye at equilibrium, q_e (mg/g) is the corresponding adsorption capacity. Q_m (mg/g) is the theoretical maximum adsorption capacity of adsorbents, K_L (L/mg) is the Langmuir isotherm coefficients related to the free energy of adsorption, K_F ((mg/g)(L/mg)$^{1/n}$) and $1/n$ are the adsorption constants of Freundlich model.

The adsorption isotherm parameters of K-2BP dye adsorption by four kinds of adsorbents are listed in Table 3.

The values of correlation coefficient R^2 for Freundlich model of K-2BP dye adsorption on MNS, EMNS, DMNS and TMNS (0.9129, 0.9568, 0.9831 and 0.9679, respectively) were higher than that of Langmuir model, indicating that the Freundlich model is more fitted to characterize the equilibrium adsorption. This was constant with multilayer adsorption due to the presence of energetically heterogeneous adsorption sites. In general, values $1/n < 1$ illustrated that adsorbate was favorably adsorbed onto adsorbent [67,68].

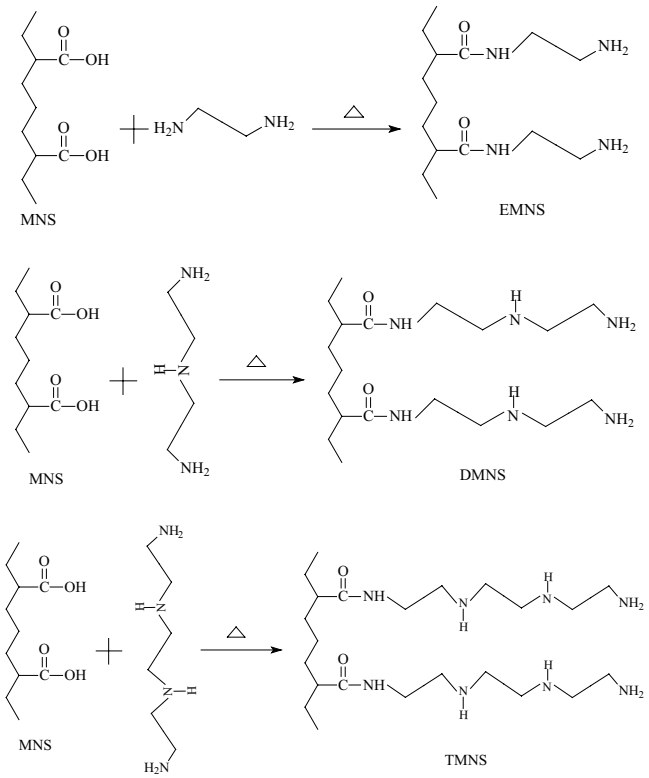

Fig. 10. Associated reactions of the chemical modification process.

4. Conclusion

In this work, the raw MNS, and the ethylenediamine, diethylenetriamine and triethylenetetramine modified MNS were used to remove K-2BP dye from aqueous solutions. The raw MNS, and the ethylenediamine, diethylenetriamine and triethylenetetramine modified MNS (EMNS, DMNS and TMNS) are porous, multilayer and tubular structures with average particle sizes of 84.497, 109.098, 121.400 and 113.006 μm, respectively. The band generated at 1,335 and

Table 3
Adsorption isotherm constants for K-2BP adsorption onto the adsorbents (MNS, EMNS, DMNS, TMNS) (conditions: temperature, 25°C; stirring rate, 180 rpm; reaction time, 180 min; pH, 6.91)

Isotherm models	Parameters	MNS	EMNS	DMNS	TMNS
Langmuir	Q_m (mg/g)	49.7512	85.4701	128.2051	125.0000
	K_L (L/mg)	0.0120	0.0147	0.0299	0.0389
	R^2	0.8534	0.8125	0.9047	0.8906
Freundlich	K_F ((mg/g)(L/mg)$^{1/n}$)	1.0226	2.1596	9.3194	11.3748
	$1/n$	0.7050	0.6847	0.4991	0.4662
	R^2	0.9129	0.9568	0.9832	0.9679

1,225 cm^{-1} caused by C–N bend vibrations in amino group and amide group indicated that amine groups were grafted on the surface of MNS after modification. The influence of pH on K-2BP dye removal indicated that the existence of amino groups in adsorbents enhanced their absorption capabilities. Moreover, it was demonstrated that the adsorption processes were spontaneous and endothermic. The adsorption kinetics of pristine and functionalized adsorbents were well described by the pseudo-second-order kinetic model, suggesting that the adsorption of K-2BP dye on adsorbents was chemisorption and the rate-limiting step might be the electrostatic and hydrogen bonding interaction. In addition, the adsorption kinetics was well confirmed with the pseudo-second-order equation. When the total numbers of amino modifying were the same, the adsorption equilibrium rates reached the same constant value. If the amino numbers were different, less time was needed for the modifiers with more amino numbers per mol to get the adsorption equilibrium rate constant. The variation of h values indicated that by increasing amino groups per mole modifiers, the initial adsorption rate could be higher. As a result, MNSs modified with more amino groups showed a better performance in removing azo dye reactive brilliant red (K-2BP) in printing and dyeing wastewater.

Acknowledgments

This work was supported by the National Natural Science Foundation of China (51579072 and 51208173), the Fundamental Research Funds for the Central Universities (2017B13314), the Priority Academic Program Development of Jiangsu Higher Education Institutions (PAPD), the Major Science and Technology Program for Water Pollution Control and Treatment (2014ZX07305-002), the Water Conservancy Science Technology Project of Jiangsu Province (2016040 and 2017047), the Ningbo Science and Technology Plan Project (2017A80002), the Ningbo Science and Technology benefit people Project (2017C50002).

References

[1] V.K. Gupta, Suhas, Application of low-cost adsorbents for dye removal--a review, J. Environ. Manage., 90 (2009) 2313–2342.
[2] V.M. Vučurović, R.N. Razmovski, U.D. Miljić, V.S. Puškaš, Removal of cationic and anionic azo dyes from aqueous solutions by adsorption on maize stem tissue, J. Taiwan Inst. Chem. Eng., 45 (2014) 1700–1708.
[3] V.O. Njoku, K.Y. Foo, M. Asif, B.H. Hameed, Preparation of activated carbons from rambutan (*Nephelium lappaceum*) peel by microwave-induced KOH activation for acid yellow 17 dye adsorption, Chem. Eng. J., 250 (2014) 198–204.
[4] S.S. Madaeni, Z. Jamali, N. Islami, Highly efficient and selective transport of methylene blue through a bulk liquid membrane containing Cyanex 301 as carrier, Sep. Purif. Technol., 6 (2011) 631–638.
[5] A. Mittal, D. Kaur, A. Malviya, J. Mittal, V.K. Gupta, Adsorption studies on the removal of coloring agent phenol red from wastewater using waste materials as adsorbents, J. Colloid Interface Sci., 337 (2009) 345–354.
[6] Y. Hu, G. Tan, X. Ye, L. Quan, G. Min, H. Liu, Z. Wu, Dye adsorption by resins: effect of ionic strength on hydrophobic and electrostatic interactions, Chem. Eng. J., 228 (2013) 392–397.
[7] T.A. Saleh, V.K. Gupta, Column with CNT/magnesium oxide composite for lead (II) removal from water, Environ. Sci. Pollut. Res., 19 (2012) 1224–1228.
[8] S. Wongcharee, V. Aravinthan, L. Erdei, W. Sanongraj, Mesoporous activated carbon prepared from macadamia nut shell waste by carbon dioxide activation: comparative characterisation and study of methylene blue removal from aqueous solution, Asia-pacific J. Chem. Eng., 13 (2018) e2179.
[9] L.A. Rodrigues, G.P. Thim, R.R. Ferreira, M.O. Alvarez-Mendez, A.D.R. Coutinho, Activated carbon derived from macadamia nut shells: an effective adsorbent for phenol removal, J. Porous Mater., 20 (2013) 619–627.
[10] G.E.J. Poinern, G. Senanayake, N. Shah, T.L. Xuan, G.M. Parkinson, D. Fawcett, Adsorption of the aurocyanide, complex on granular activated carbons derived from macadamia nut shells – a preliminary study, Miner. Eng., 24 (2011) 1694–1702.
[11] A.C. Martins, O. Pezoti, A.L. Cazetta, K.C. Bedin, D.A.S. Yamazaki, G.F.G. Bandoch, T. Asefa, J.V. Visentainer, V.C. Almeida, Removal of tetracycline by NaOH-activated carbon produced from macadamia nut shells: kinetic and equilibrium studies, Chem. Eng. J., 260 (2015) 291–299.
[12] V.E. Pakade, L.C. Maremeni, T.D. Ntuli, N.T. Tavengwa, Application of quaternized activated carbon derived from macadamia nutshells for the removal of hexavalent chromium from aqueous solutions, South Afr. J. Chem., 69 (2016) 180–188.
[13] C. Du, Y. Xue, Z. Wu, Z. Wu, Microwave assisted one-step preparation of macadamia nuts shell based activated carbon for efficient adsorption of Reactive Blue, New J. Chem., 41 (2017) 15373–15383.
[14] O.P. Junior, A.L. Cazetta, R.C. Gomes, É.O. Barizão, I.P.A.F. Souza, A.C. Martins, T. Asefa, V.C. Almeida, Synthesis of $ZnCl_2$ -activated carbon from macadamia nut endocarp (*Macadamia integrifolia*) by microwave-assisted pyrolysis: optimization using RSM and methylene blue adsorption, J. Anal. Appl. Pyrolysis, 105 (2014) 166–176.
[15] M. Danish, T. Ahmad, A review on utilization of wood biomass as a sustainable precursor for activated carbon production and application, Renew. Sustain. Energy Rev., 87 (2018) 1–21.
[16] L.C. Maremeni, S.J. Modise, F.M. Mtunzi, M.J. Klink, V.E. Pakade, adsorptive removal of hexavalent chromium

by diphenylcarbazide-grafted macadamia nutshell powder, Bioinorg. Chem. Appl., 2018 (2018) 1–14.
[17] P.M.K. Reddy, K. Krushnamurty, S.K. Mahammadunnisa, A. Dayamani, C. Subrahmanyam, Preparation of activated carbons from bio-waste: effect of surface functional groups on methylene blue adsorption, Int. J. Environ. Sci. Technol., 12 (2015) 1363–1372.
[18] Y. Zeng, L. Prasetyo, V.T. Nguyen, T. Horikawa, D.D. Do, D. Nicholson, Characterization of oxygen functional groups on carbon surfaces with water and methanol adsorption, Carbon, 81 (2015) 447–457.
[19] G.X. Yang, H. Jiang, Amino modification of biochar for enhanced adsorption of copper ions from synthetic wastewater, Water Res., 48 (2014) 396–405.
[20] Y. Ma, W.J. Liu, N. Zhang, Y.S. Li, H. Jiang, G.P. Sheng, Polyethylenimine modified biochar adsorbent for hexavalent chromium removal from the aqueous solution, Bioresour. Technol., 169 (2014) 403–408.
[21] J.S. Cao, J.X. Lin, F. Fang, M.T. Zhang, Z.R. Hu, A new absorbent by modifying walnut shell for the removal of anionic dye: kinetic and thermodynamic studies, Bioresour. Technol., 163 (2014) 199–205.
[22] B.H. Hameed, H. Hakimi, Utilization of durian (*Durio zibethinus* Murray) peel as low cost sorbent for the removal of acid dye from aqueous solutions, Biochem. Eng. J., 39 (2008) 338–343.
[23] J. Yang, K. Qiu, Preparation of activated carbons from walnut shells via vacuum chemical activation and their application for methylene blue removal, Chem. Eng. J., 165 (2010) 209–217.
[24] L.S. Coulibaly, S.K. Akpo, J. Yvon, L. Coulibaly, Fourier transform infra-red (FTIR) spectroscopy investigation, dose effect, kinetics and adsorption capacity of phosphate from aqueous solution onto laterite and sandstone, J. Environ. Manage., 183 (2016) 1032.
[25] G.Z. Kyzas, P.I. Siafaka, E.G. Pavlidou, K.J. Chrissafis, D.N. Bikiaris, Synthesis and adsorption application of succinyl-grafted chitosan for the simultaneous removal of zinc and cationic dye from binary hazardous mixtures, Chem. Eng. J., 259 (2015) 438–448.
[26] V. Nair, A. Panigrahy, R. Vinu, Development of novel chitosan–lignin composites for adsorption of dyes and metal ions from wastewater, Chem. Eng. J., 254 (2014) 491–502.
[27] Z. Li, X. Tang, K. Liu, J. Huang, Q. Peng, M. Ao, Z. Huang, Fabrication of novel sandwich nanocomposite as an efficient and regenerable adsorbent for methylene blue and Pb (II) ion removal, J. Environ. Manage., 218 (2018) 363–373.
[28] W. Shen, Z. Li, Y. Liu, Surface chemical functional groups modification of porous carbon, Recent Patents Chem. Eng., 1 (2008) 27–40.
[29] S. Hassan, L. Duclaux, J.M. Lévêque, L. Reinert, A. Farooq, T. Yasin, Effect of cation type, alkyl chain length, adsorbate size on adsorption kinetics and isotherms of bromide ionic liquids from aqueous solutions onto microporous fabric and granulated activated carbons, J. Environ. Manage., 144 (2014) 108–117.
[30] Y. Ping, T. Yuan, Z. Wang, R. Qu, X. Liu, X. Qiang, Q. Tang, Synthesis of functionalized silica gel with poly (diethylenetriamine bis (methylene phosphonic acid)) and its adsorption properties of transition metal ions, Mater. Chem. Phys., 129 (2011) 168–175.
[31] F.M.D. Oliveira, B.F. Somera, M.Z. Corazza, M.J.S. Yabe, M.G. Segatelli, E.S. Ribeiro, É.C. Lima, S.L.P. Dias, C.R.T. Tarley, Cellulose microfiber functionalized with N,N′-bis (2-aminoethyl)-1,2-ethanediamine as a solid sorbent for the fast preconcentration of Cd(II) in flow system analysis, Talanta, 85 (2011) 2417–2424.
[32] R. Bhattacharyya, S.K. Ray, Removal of congo red and methyl violet from water using nano clay filled composite hydrogels of poly acrylic acid and polyethylene glycol, Chem. Eng. J., 260 (2015) 269–283.
[33] Ş. Taşar, F. Kaya, A. Özer, Biosorption of lead (II) ions from aqueous solution by peanut shells: Equilibrium, thermodynamic and kinetic studies, J. Environ. Chem. Eng., 2 (2014) 1018–1026.
[34] R. Gong, Y. Sun, J. Chen, H. Liu, C. Yang, Effect of chemical modification on dye adsorption capacity of peanut hull, Dyes Pigm., 67 (2006) 175–181.
[35] T. Altun, E. Pehlivan, Removal of Cr (VI) from aqueous solutions by modified walnut shells, Food Chem., 132 (2012) 693–700.
[36] T.H. Liou, Development of mesoporous structure and high adsorption capacity of biomass-based activated carbon by phosphoric acid and zinc chloride activation, Chem. Eng. J., 158 (2010) 129–142.
[37] R.H. Hesas, A. Arami-Niya, M.A.W.D. Wan, J.N. Sahu, Preparation of granular activated carbon from oil palm shell by microwave-induced chemical activation: optimisation using surface response methodology, Chem. Eng. Res. Des., 91 (2013) 2447–2456.
[38] A. Khan, S. Badshah, C. Airoldi, Biosorption of some toxic metal ions by chitosan modified with glycidylmethacrylate and diethylenetriamine, Chem. Eng. J., 171 (2011) 159–166.
[39] K. Fujiwara, A. Ramesh, T. Maki, H. Hasegawa, K. Ueda, Adsorption of platinum (IV), palladium (II) and gold (III) from aqueous solutions onto L-lysine modified crosslinked chitosan resin, J. Hazard. Mater., 146 (2007) 39–50.
[40] T.S. Anirudhan, P.S. Suchithra, S. Rijith, Amine–modified polyacrylamide–bentonite composite for the adsorption of humic acid in aqueous solutions, Colloids Surf., A, 326 (2008) 147–156.
[41] H. Li, S. Bi, L. Liu, W. Dong, X. Wang, Separation and accumulation of Cu(II), Zn(II) and Cr(VI) from aqueous solution by magnetic chitosan modified with diethylenetriamine, Desalination, 278 (2011) 397–404.
[42] C.H. Xiong, C.P. Yao, Synthesis, characterization and application of triethylenetetramine modified polystyrene resin in removal of mercury, cadmium and lead from aqueous solutions, Chem. Eng. J., 155 (2009) 844–850.
[43] C. Gruian, E. Vanea, S. Simon, V. Simon, FTIR and XPS studies of protein adsorption onto functionalized bioactive glass, Biochim. Biophys. Acta, 1824 (2012) 873.
[44] M. Carrier, A. Loppinetserani, D. Denux, J.M. Lasnier, F. Hampichavant, F. Cansell, C. Aymonier, Thermogravimetric analysis as a new method to determine the lignocellulosic composition of biomass, Biomass Bioenergy, 35 (2011) 298–307.
[45] J. Lédé, Cellulose pyrolysis kinetics: an historical review on the existence and role of intermediate active cellulose, J. Anal. Appl. Pyrolysis, 94 (2012) 17–32.
[49] Z. Luo, S. Wang, X. Guo, Selective pyrolysis of Organosolv lignin over zeolites with product analysis by TG-FTIR, J. Anal. Appl. Pyrolysis, 95 (2012) 112–117.
[47] S. Chen, Q. Yue, B. Gao, X. Xing, Equilibrium and kinetic adsorption study of the adsorptive removal of Cr(VI) using modified wheat residue, J. Colloid Interface Sci., 349 (2010) 256.
[48] Y.R. Zhang, P. Su, J. Huang, Q.R. Wang, B.X. Zhao, A magnetic nanomaterial modified with poly-lysine for efficient removal of anionic dyes from water, Chem. Eng. J., 262 (2015) 313–318.
[49] C. Namasivayam, D. Kavitha, Removal of Congo Red from water by adsorption onto activated carbon prepared from coir pith, an agricultural solid waste, Dyes Pigm., 54 (2002) 47–58.
[50] D. Bilba, D. Suteu, T. Malutan, Removal of reactive dye brilliant red HE-3B from aqueous solutions by hydrolyzed polyacrylonitrile fibres: equilibrium and kinetics modelling, Open Chem., 6 (2008) 258.
[51] W. Jingang, W. Xikui, G. Peiquan, Y. Jiemei, Degradation of reactive brilliant red K-2BP in aqueous solution using swirling jet-induced cavitation combined with H2O2, Ultrason. Sonochem., 18 (2011) 494–500.
[52] S. Canzano, P. Iovino, S. Salvestrini, S. Capasso, Comment on Removal of anionic dye Congo red from aqueous solution by raw pine and acid-treated pine cone powder as adsorbent: equilibrium, thermodynamic, kinetics, mechanism and process design, Water Res., 46 (2012) 4314–4315.
[53] D. Suteu, T. Malutan, D. Bilba, Removal of reactive dye Brilliant Red HE-3B from aqueous solutions by industrial lignin: Equilibrium and kinetics modeling, Desalination, 255 (2010) 84–90.

[54] C. Zhang, S. Yang, H. Chen, H. He, C. Sun, Adsorption behavior and mechanism of reactive brilliant red X-3B in aqueous solution over three kinds of hydrotalcite-like LDHs, Appl. Surf. Sci., 301 (2014) 329–337.
[55] J. Fu, Z. Chen, M. Wang, S. Liu, J. Zhang, J. Zhang, R. Han, Q. Xu, Adsorption of methylene blue by a high-efficiency adsorbent (polydopamine microspheres): kinetics, isotherm, thermodynamics and mechanism analysis, Chem. Eng. J., 259 (2015) 53–61.
[56] L. Yu, Y.M. Luo, The adsorption mechanism of anionic and cationic dyes by Jerusalem artichoke stalk-based mesoporous activated carbon, J. Environ. Chem. Eng., 2 (2014) 220–229.
[57] C. Kotsmar, V. Pradines, V.S. Alahverdjieva, E.V. Aksenenko, V.B. Fainerman, V.I. Kovalchuk, J. Krägel, M.E. Leser, B.A. Noskov, R. Miller, Thermodynamics, adsorption kinetics and rheology of mixed protein-surfactant interfacial layers, Adv. Colloid Interface Sci., 150 (2009) 41–54.
[58] M. Nas, R.A. Abu-Zurayk, I. Hamadneh, A.H. Al-Dujaili, Phenol adsorption on biochar prepared from the pine fruit shells: equilibrium, kinetic and thermodynamics studies, J. Environ. Manage., 226 (2018) 377.
[59] K.Y. Chong, C.H. Chia, S. Zakaria, M.S. Sajab, Vaterite calcium carbonate for the adsorption of Congo red from aqueous solutions, J. Environ. Chem. Eng., 2 (2014) 2156–2161.
[60] G. Moussavi, R. Khosravi, The removal of cationic dyes from aqueous solutions by adsorption onto pistachio hull waste, Chem. Eng. Res. Des., 89 (2011) 2182–2189.
[61] P. Luo, Y. Zhao, B. Zhang, J. Liu, Y. Yang, J. Liu, Study on the adsorption of Neutral Red from aqueous solution onto halloysite nanotubes, Water Res., 44 (2010) 1489.
[62] P. Liao, Z.M. Ismael, W. Zhang, S. Yuan, M. Tong, K. Wang, J. Bao, Adsorption of dyes from aqueous solutions by microwave modified bamboo charcoal, Chem. Eng. J., 195–196 (2012) 339–346.
[63] W.C. Wanyonyi, J.M. Onyari, P.M. Shiundu, Adsorption of Congo Red dye from aqueous solutions using roots of *Eichhornia crassipes*: kinetic and equilibrium studies, Energy Procedia, 50 (2014) 862–869.
[64] A.B. Albadarin, J. Mo, Y. Glocheux, S. Allen, G. Walker, C. Mangwandi, Preliminary investigation of mixed adsorbents for the removal of copper and methylene blue from aqueous solutions, Chem. Eng. J., 255 (2014) 525–534.
[75] N. Deihimi, M. Irannajad, B. Rezai, Equilibrium and kinetic studies of ferricyanide adsorption from aqueous solution by activated red mud, J. Environ. Manage., 227 (2018) 277.
[66] M.K. Dahri, M.R.R. Kooh, L.B.L. Lim, Water remediation using low cost adsorbent walnut shell for removal of malachite green: equilibrium, kinetics, thermodynamic and regeneration studies, J. Environ. Chem. Eng., 2 (2014) 1434–1444.
[67] W. Konicki, I. Pełech, E. Mijowska, I. Jasińska, Adsorption of anionic dye Direct Red 23 onto magnetic multi-walled carbon nanotubes-Fe_3C nanocomposite: kinetics, equilibrium and thermodynamics, Chem. Eng. J., 210 (2012) 87–95.
[68] C. Ng, J.N. Losso, W.E. Marshall, R.M. Rao, Freundlich adsorption isotherms of agricultural by-product-based powdered activated carbons in a geosmin-water system, Bioresour. Technol., 85 (2002) 131–135.